Physicochemical and electrochemical characterisation of imidazolium based IL + GBL mixtures as electrolytes for lithium-ion batteries

Supporting information

Snežana Papović[1], Nikola Cvjetićanin[2],

Slobodan Gadžurić[1], Marija Bešter-Rogač[3], Milan Vraneš[1*],

[1]*Faculty of Science, Department of Chemistry, Biochemistry and Environmental Protection, University of Novi Sad, Trg Dositeja Obradovića 3, 21000 Novi Sad, Serbia*

[2]*Faculty of Physical Chemistry, University of Belgrade, Studentski trg 12-16, 11158 Belgrade, Serbia*

[3]*Faculty of Chemistry and Chemical Technology, University of Ljubljana, Večna pot 113, 1000 Ljubljana, Slovenia*

[*] Corresponding Author: Tel: +381 21 485 2751; Fax: +381 21 454 065; E-mail: milan.vranes@dh.uns.ac.rs

Table S1. Provenance and purity of the samples.

Ionic liquid	Provenance	Product Number	Purification method	Mass fraction	KF[g] determined water content (ppm)	Halide content (ppm)
C_2mimTFSI[a]	Merck	174899-82-2	Vacuum drying	≥ 0.99	32	5
C_4mimTFSI[b]	Merck	174899-83-	Vacuum drying	≥ 0.99	62	9
C_6mimTFSI[c]	IoLiTec	382150-50-7	Vacuum drying	≥ 0.99	54	8
C_8mimTFSI[d]	IoLiTec	178631-04-4	Vacuum drying	≥ 0.99	48	10
C_2mmimTFSI[e]	IoLiTec	174899-90-2	Vacuum drying	≥ 0.99	34	8
GBL[f]	Aldrich	96-48-0	Distillation	≥ 0.99	61	-
LiTFSI[g]	Aldrich	90076-65-6	Vacuum drying	≥ 0.9995	-	-
Ti-foil	Alfa Aesar	7440-32-6	-	≥ 0.995		

[a]1-ethyl-3-methylimidazolium *bis*(trifluoromethylsulfonyl)imide
[b]1-butyl-3-methylimidazolium *bis*(trifluoromethylsulfonyl)imide
[c]1-hexyl-3-methylimidazolium *bis*(trifluoromethylsulfonyl)imide
[d]1-octyl-3-methylimidazolium *bis*(trifluoromethylsulfonyl)imide
[e]1-ethyl-2,3-dimethylimidazolium *bis*(trifluoromethylsulfonyl)imide
[f]γ-butyrolactone
[g] lithium *bis*(trifuoromethylsulfonyl)imide
[h]KF titration = Karl Fischer titration


Sample
GBL
C_2mimTFSI/GBL x_{IL}≈0.1
C_2mimTFSI/GBL x_{IL}≈0.15
a)
b)
c)
d)
e)
f)
g)
h)
0 s
10 s
20 s
30 s
40 s
50 s
60 s
80 s

Sample

C_2mimTFSI/GBL x_{IL}≈0.175 | **C_2mimTFSI/GBL x_{IL}≈0.20** | **C_2mimTFSI/GBL x_{IL}≈0.3**

Figure S1. Flammabilty test pictures of C_2mimTFSI/GBL at: a) starting time, b) after 10, c) 20, d) 30, e) 40, f) 50, g) 60 and h) after 80 seconds (x_{IL} ≈ 0.0 – 0.3; x_{IL} is mole fraction of ionic liquid C_2mimTFSI).

Table S2. Flammability test: sample initial weight, flame exposure time, flame extinguish and self-extinguish time for binary mixture C_2mimTFSI/GBL.

Sample	Sample initial weight /g	Flame exposure time / s	Flame extinguish time / s	Self-extinguishing time (SET) / $s \cdot g^{-1}$
GBL	0.2034	5	70	344.15
0.1	0.1950	5	45	230.77
0.15	0.1944	5	35	180.04
0.175	0.1965	5	31	157.76
0.2	0.1985	5	27	136.02
0.25	0.1974	5	19.42	98.38
0.3	0.1914	5	13	67.92
0.4	0.1909	5	-	-

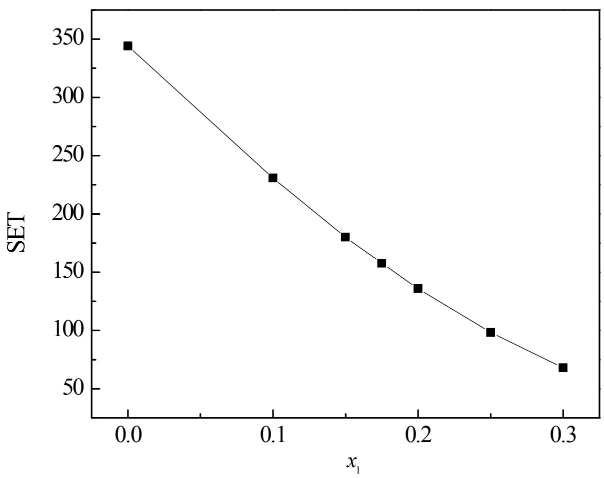

Figure S2. Increasing the amount of C_2mimTFSI/GBL ($x_{IL} \approx 0.0 – 0.3$; x_{IL} is mole fraction of IL) self-extinguishing time (SET, i.e. the flame extinguish time normalized to the weight of the samples).

Table S3. Densities, d_s, viscosities, η, and relative permittivities, ε, of GBL as a function of temperature.

T	d_s	$10^3 \cdot \eta$	ε
K	$kg \cdot dm^{-3}$	$Pa \cdot s$	
273.15	1.149155	2.69	44.4
278.15	1.144229	2.43	43.8
283.15	1.139314	2.21	43.2
288.15	1.134403	2.02	42.6
293.15	1.129493	1.86	42.0
298.15	1.124588	1.71	41.4
303.15	1.119684	1.58	40.8
308.15	1.114782	1.47	40.2
313.15	1.109874	1.37	39.6

Table S4. Densities of the final solutions (m_2) in the conductivity cell and of the stock solutions, (m_1), used for sample preparation at $T = 298.15$ K.

m	d
mol·kg^{-1}	kg·dm^{-3}
C_2mimTFSI	
(m_2) 0.004826	1.125151
(m_1) 0.09997	1.136175
C_4mimTFSI	
(m_2) 0.005761	1.125172
(m_1) 0.120012	1.137164
C_6mimTFSI	
(m_2) 0.004763	1.125045
(m_1) 0.097064	1.133540
C_8mimTFSI	
(m_2) 0.00543	1.1245880
(m_1) 0.09678	1.1324420

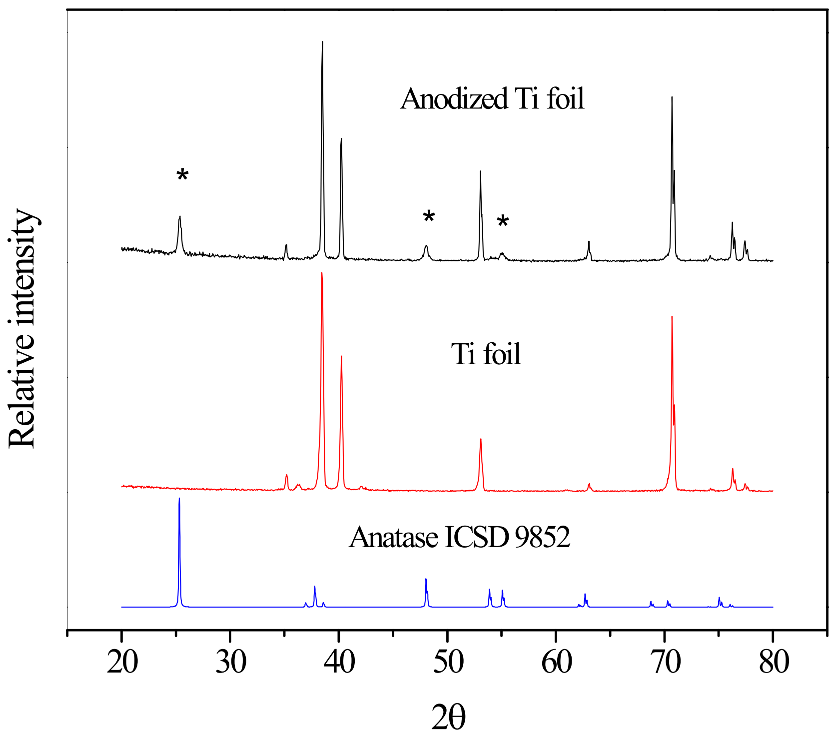

Figure S3. *X*-ray diffraction data before and after anodization.

(a)

(b)

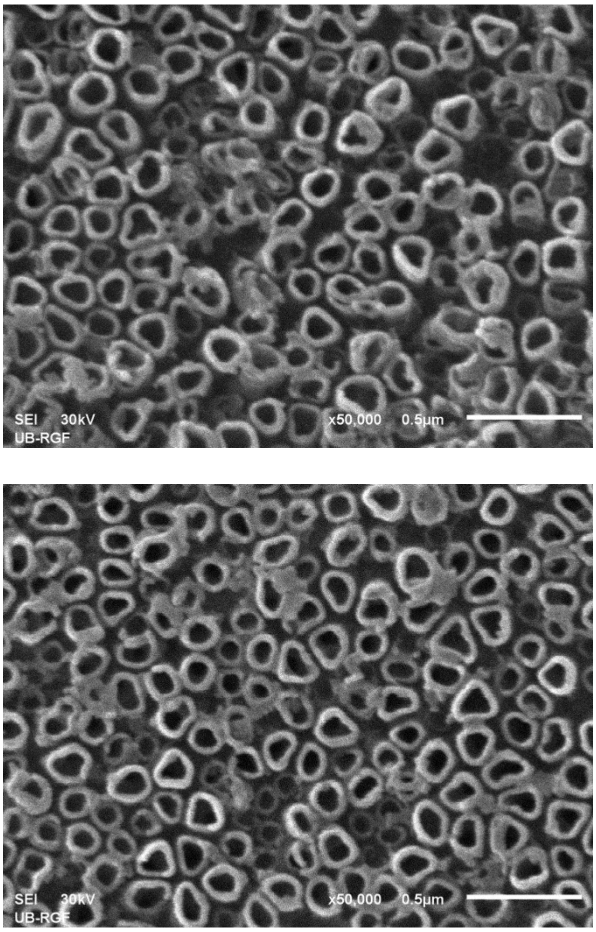

Figure S4. SEM images of TiO_2 NTAs: (a) before and (b) after cycling.

Table S5. Molar conductivities (Λ) as a function of IL molality, m, and density gradients, b, for C_2mimTFSI, C_4mimTFSI, C_6mimTFSI and C_8mimTFSI in GBL binary mixtures at temperature range (273.15 – 313.15) K.

	T / K								
$10^3 \cdot m$ mol·kg^{-1}	273.15	278.15	283.15	288.15	293.15	298.15	303.15	308.15	313.15
	Λ / S·cm^2·dm^{-3}·mol^{-1}								
	C_2mimTFSI b / kg^2·dm^{-3}·mol^{-1} = 0.0766								
0.8329	25.638	28.245	30.971	33.715	36.445	39.275	42.347	45.709	48.955
1.2429	25.373	27.931	30.600	33.309	36.099	38.983	42.035	45.291	48.493
1.7509	25.131	27.658	30.297	32.998	35.799	38.677	41.711	44.889	48.059
2.3261	24.909	27.459	30.079	32.731	35.493	38.358	41.351	44.476	47.610
3.0487	24.661	27.169	29.756	32.399	35.169	38.019	40.977	44.047	47.142
3.7740	24.457	26.932	29.479	32.149	34.894	37.723	40.652	43.687	46.764
4.4812	24.299	26.770	29.335	31.979	34.674	37.461	40.365	43.368	46.418
5.2629	24.134	26.584	29.131	31.751	34.432	37.214	40.091	43.069	46.091
	273.15	278.15	283.15	288.15	293.15	298.15	303.15	308.15	313.15
	C_4mimTFSI b / kg^2·dm^{-3}·mol^{-1} = 0.0912								
0.4399	24.001	26.474	29.055	31.743	34.391	36.900	39.790	43.000	46.100
0.7837	23.809	26.255	28.798	31.455	34.124	36.688	39.533	42.660	45.707
1.1181	23.551	25.966	28.480	31.095	33.753	36.364	39.174	42.214	45.216
1.6369	23.281	25.663	28.153	30.716	33.392	36.065	38.786	41.749	44.686
2.3429	23.016	25.363	27.814	30.344	32.967	35.659	38.457	41.376	44.217
3.2381	22.789	25.115	27.544	30.047	32.640	35.305	38.070	40.942	43.756
4.0907	22.627	24.922	27.327	29.810	32.382	35.028	37.768	40.582	43.359
4.9423	22.439	24.736	27.124	29.591	32.146	34.771	37.489	40.273	43.051
5.7481	22.285	24.566	26.921	29.387	31.916	34.539	37.292	39.941	42.747
6.5959	24.001	26.474	29.055	31.743	34.391	36.900	39.790	43.000	46.100
$10^3 \cdot m$	273.15	278.15	283.15	288.15	293.15	298.15	303.15	308.15	313.15
	C_6mimTFSI b / kg^2·dm^{-3}·mol^{-1} = 0.0915								
0.7078	22.913	25.304	27.764	30.332	32.851	35.176	37.819	40.599	43.559
1.0878	22.677	25.029	27.480	29.953	32.381	34.878	37.585	40.361	43.275
0.3835	22.479	24.804	27.214	29.721	32.209	34.686	37.355	40.113	42.988
1.4960	22.306	24.610	26.978	29.395	31.851	34.429	37.108	39.852	42.704
1.9620	22.102	24.376	26.744	29.161	31.589	34.152	36.811	39.534	42.351
2.5666	21.883	24.132	26.464	28.882	31.397	33.916	36.472	39.158	41.944
3.3496	21.703	23.933	26.251	28.629	31.045	33.569	36.181	38.855	41.613
4.0526	21.543	23.755	26.053	28.431	30.861	33.340	35.926	38.584	41.322
4.7705	21.403	23.594	25.851	28.188	30.622	33.132	35.705	38.347	41.068
5.4755	22.913	25.304	27.764	30.332	32.851	35.176	37.819	40.599	43.559
$10^3 \cdot m$	273.15	278.15	283.15	288.15	293.15	298.15	303.15	308.15	313.15
	C_8mimTFSI b / kg^2·dm^{-3}·mol^{-1} = 0.0808								
0.9057	21.903	24.164	26.586	29.156	31.552	33.961	36.562	39.271	42.053
1.2989	21.704	23.938	26.318	28.831	31.250	33.640	36.234	38.919	41.679
1.7228	21.526	23.745	26.084	28.538	31.001	33.431	35.874	38.627	41.346
2.1421	21.377	23.575	25.887	28.321	30.763	33.215	35.705	38.342	41.057

2.7114	21.178	23.323	25.566	27.997	30.376	32.836	35.391	38.010	40.703
3.3283	21.009	23.140	25.367	27.754	30.105	32.570	35.106	37.705	40.376
4.0312	20.841	22.967	25.169	27.482	29.859	32.302	34.817	37.395	40.045
4.7427	20.685	22.810	25.029	27.317	29.644	32.067	34.560	37.119	39.741
5.4578	20.544	22.654	24.852	27.124	29.445	31.850	34.325	36.867	39.479
6.2480	20.395	22.491	24.683	26.944	29.250	31.631	34.094	36.615	39.206

Relative standard uncertainties: $u_r(\kappa)$=0.05; $u_r(p)$= 0.015;
Standard uncertainties: $u(T)$ = 0.015 K; $u(m) = 3.5 \cdot 10^{-4} \text{mol} \cdot \text{kg}^{-1}$

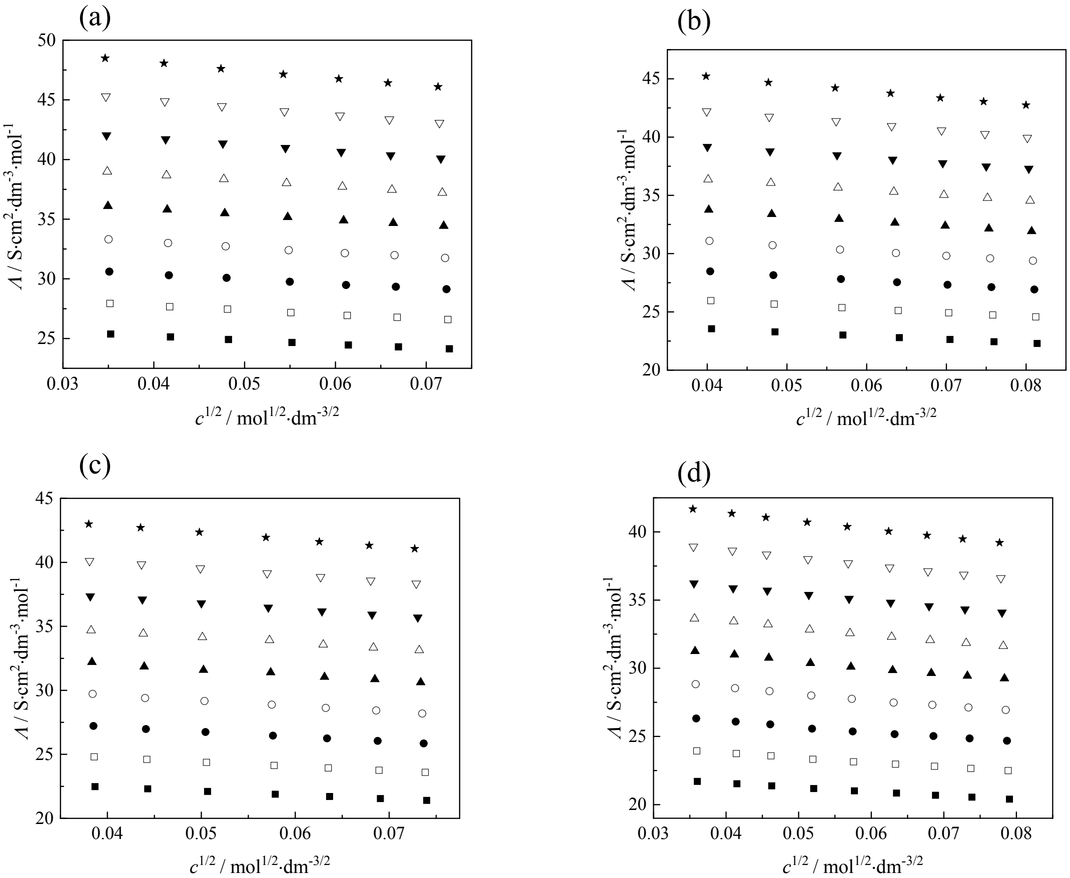

Figure S5. Molar conductivities, Λ, of ionic liquid: (a) C_2mimTFSI, (b) C_4mimTFSI, (c) C_6mimTFSI and (d) C_8mimTFSI solutions in GBL versus the square root of the molar concentration ($c^{1/2}$) from T = (273.15 – 313.15) K in steps of 5 K.

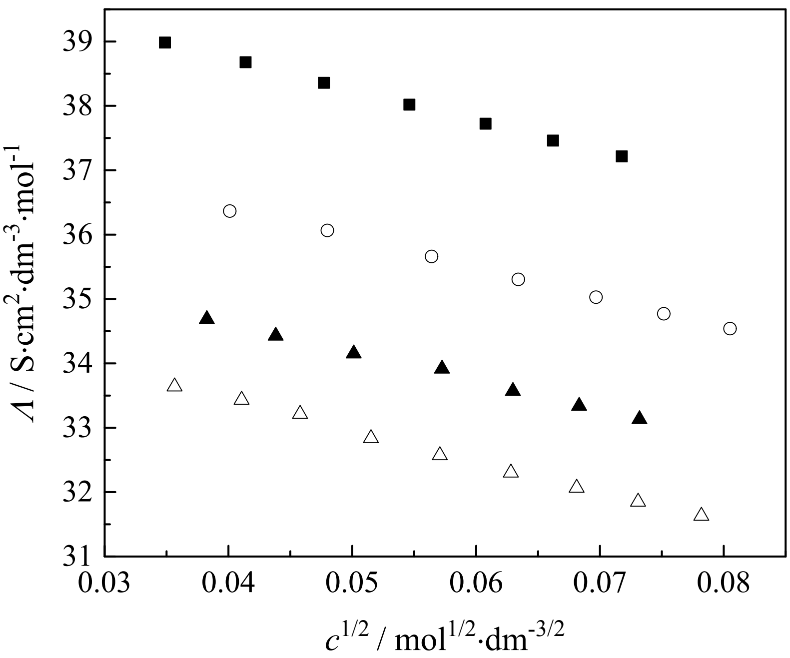

Figure S6. Comparison of molar conductivities (Λ) for: (O) C_2mimTFSI, (ꝏ) C_4mimTFSI, (□) C_6mimTFSI and (❒) C_8mimTFSI in GBL at T = 298.15 K.

Table S6. The values of standard Gibbs free energy ($\Delta G_A°$) calculated from association of ILs C_2mimTFSI, C_4mimTFSI, C_6mimTFSI and C_8mimTFSI in GBL.

T / K	$\Delta G_A°$ / J·mol^{-1}			
	C_2mimTFSI	C_4mimTFSI	C_6mimTFSI	C_8mimTFSI
273.15	-3.286	-3.863	-4.110	-4.080
278.15	-3.357	-3.980	-4.219	-4.202
283.15	-3.423	-4.150	-4.337	-4.347
288.15	-3.489	-4.324	-4.542	-4.558
293.15	-3.555	-4.431	-4.718	-4.701
298.15	-3.621	-4.594	-4.873	-4.894
303.15	-3.688	-4.737	-5.031	-5.088
308.15	-3.761	-4.862	-5.124	-5.220
313.15	-3.828	-4.987	-5.325	-5.381

Table S7. Values of α and R^2 derived from eq. (7) of different electrolytes.

Electrolyte	α	R^2
0.1 mol·dm^{-3} LiTFSI/C_2mimTFSI/GBL	0.7470	0.9972
0.25 mol·dm^{-3} LiTFSI/C_2mimTFSI/GBL	0.7552	0.9968
0.5 mol·dm^{-3} LiTFSI/C_2mimTFSI/GBL	0.8339	0.9997
0.75 mol·dm^{-3} LiTFSI/C_2mimTFSI/GBL	0.8403	0.9997
1.0 mol·dm^{-3} LiTFSI/C_2mimTFSI/GBL	0.8421	0.9998
C_2mimTFSI/GBL	0.9650	0.9941

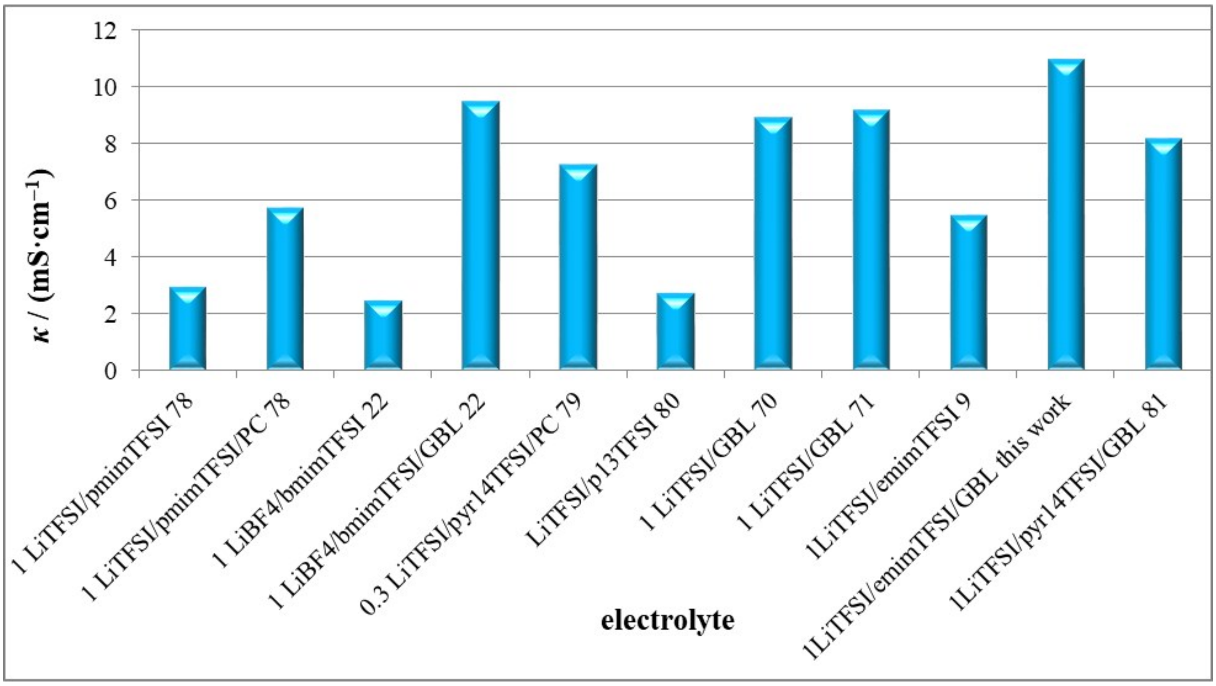

Figure S7. Comparison of the electrical conductivity values at T = 298.15 K for investigated electrolyte and similar electrolytes*9,22,70,71,78-81 at optimal compositions for LIBs.
*References are from Manuscript

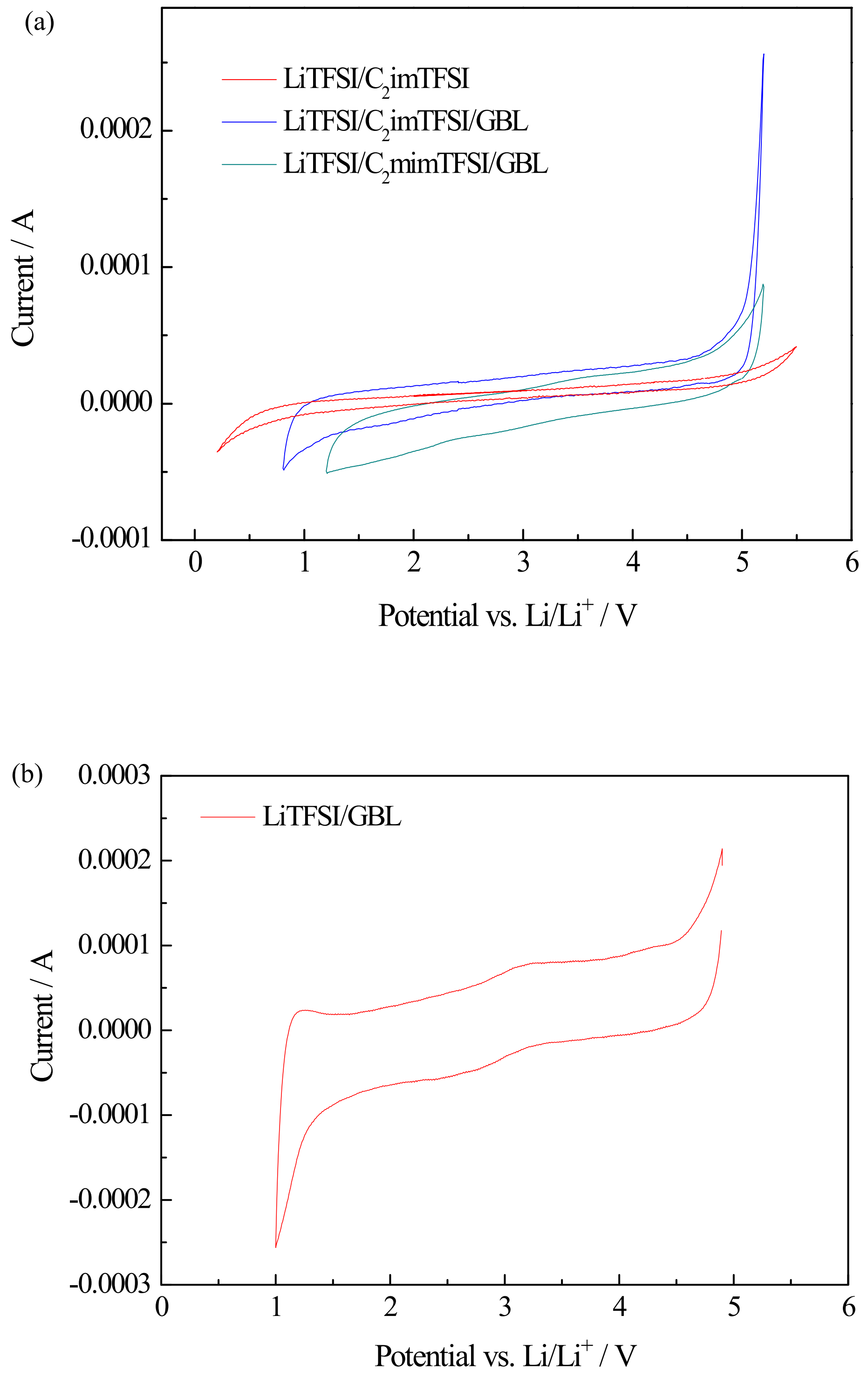

Figure S8. Electrochemical stability window of electrolytes: (a) LiTFSI/C2mimTFSI, LiTFSI/C2mimTFSI/GBL and LiTFSI/C2mmimTFSI/GBL and (b) LiTFSI/GBL on a glassy carbon working electrode and lithium metal foil as counter and reference electrode, under a scan rate of 50 mV·s-1 at T = 298.15 K.

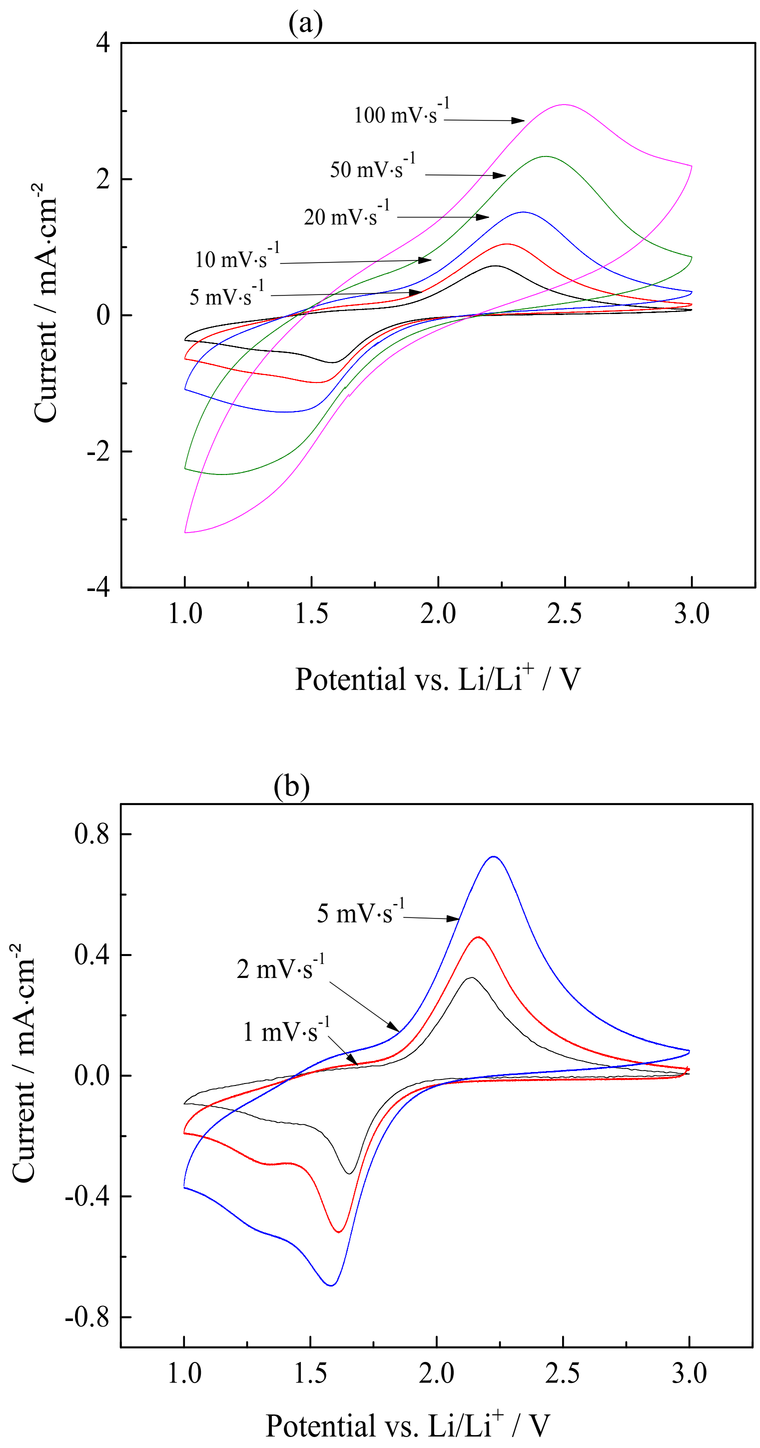

Figure S9. Cyclic voltammograms of anatase TiO_2 NTAs in LiTFSI/C_2mimTFSI electrolyte recorded at: (a) 5, 10, 20, 50 and 100 mV·s^{-1} and (b) 1, 2 and 5 mV·s^{-1} at T = 298.15 K.

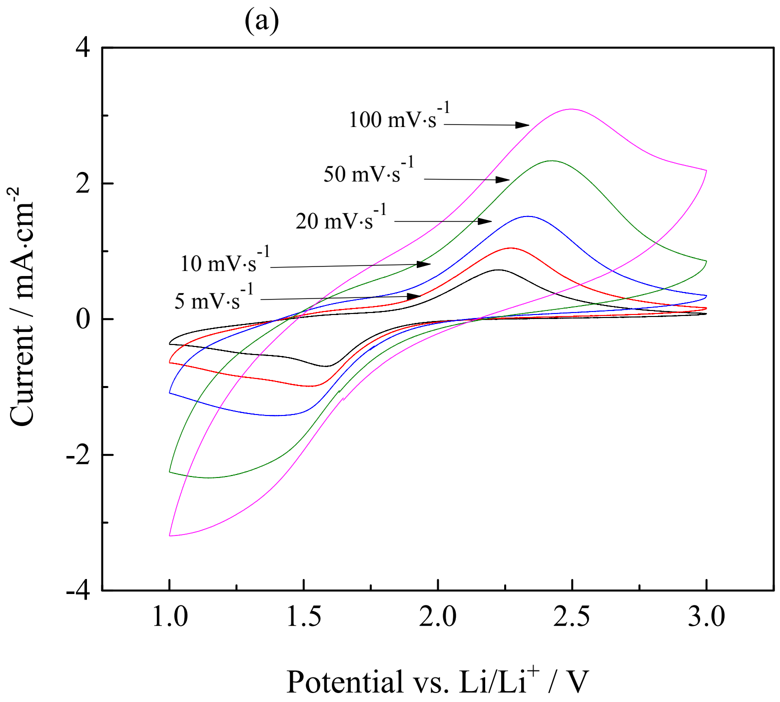

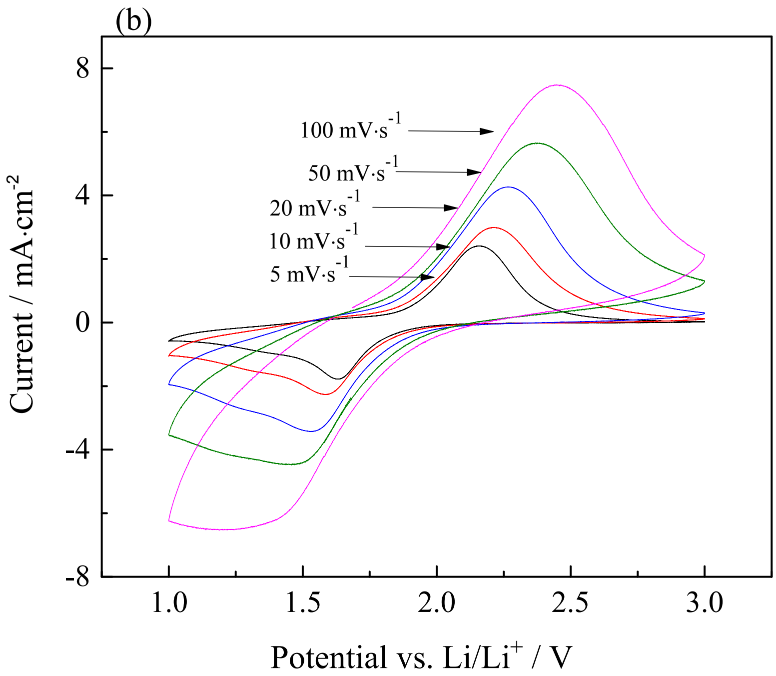

Figure S10. Cyclic voltammograms of anatase TiO2 NTAs in LiTFSI/C2mimTFSI electrolyte recorded at various scan rates (5, 10, 20, 50 and 100 mV·s–1) at temperatures T = : (a) 298.15 K and (b) 328.15 K.

Table S8. Peak-to-peak separation ΔEp at different temperatures.

T / K	ΔEp / V				
	5 mV·s-1	10 mV·s-1	20 mV·s-1	50 mV·s-1	100 mV·s-1
	LiTFSI/C2mimTFSI/GBL*				
298.15	0.59	0.66	0.75	0.88	1.06
308.15	0.51	0.58	0.67	0.80	0.93
318.15	0.46	0.52	0.60	0.74	0.87
328.15	0.41	0.48	0.56	0.70	0.83
	LiTFSI/C2mimTFSI				
298.15	0.65	0.74	0.88	1.05	1.13
308.15	0.60	0.70	0.81	0.95	1.11
318.15	0.56	0.65	0.75	0.91	1.07
328.15	0.52	0.63	0.73	0.89	1.05

*Presented in this Manuscript and presented here for comparison of ΔEp for electrolyte with and without GBL

(a)

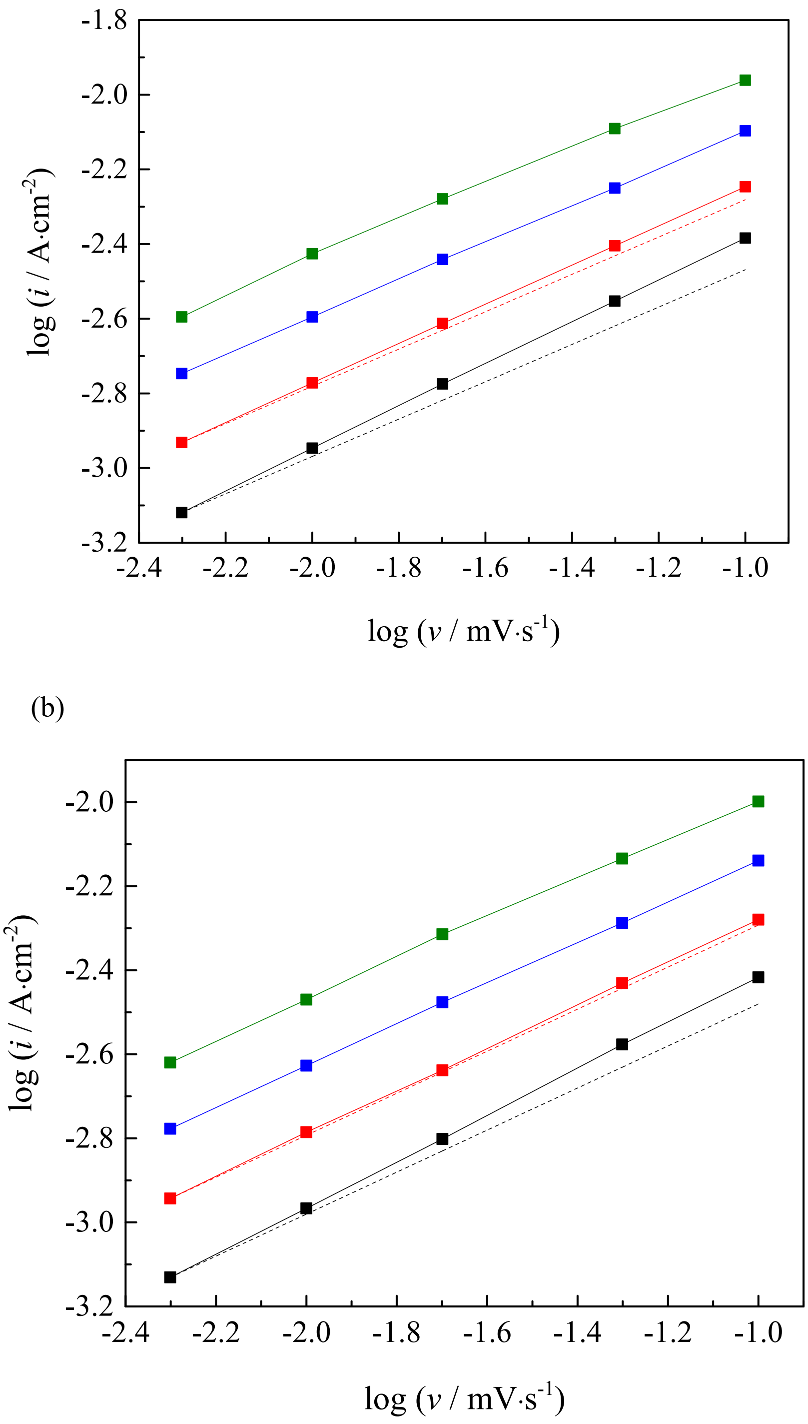

Figure S11. The relations between the current density peaks and scan rate ($\log i_p$ vs. $\log \upsilon$) of Li/TiO_2 NTAs tested in: (a) LiTFSI/C_2mimTFSI/GBL and (b) LiTFSI/C_2mmimTFSI/GBL electrolyte before (dashed line) and after (solid line) capacitive current correction.

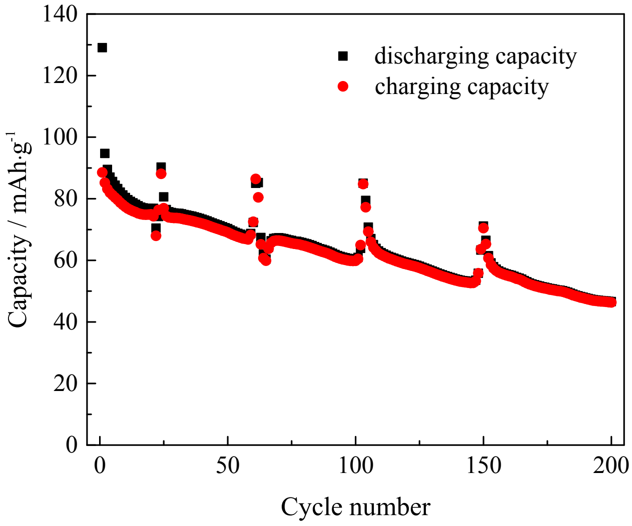

Figure S12. Charge/discharge performance of anatase TiO2 NTAs in LiTFSI/C2mimTFSI electrolyte at current rate of 1.5 C. Peaks originate from the periodic exposure of the bottle-type cell, in laboratory, to indirect sun light during daily variation of temperature.

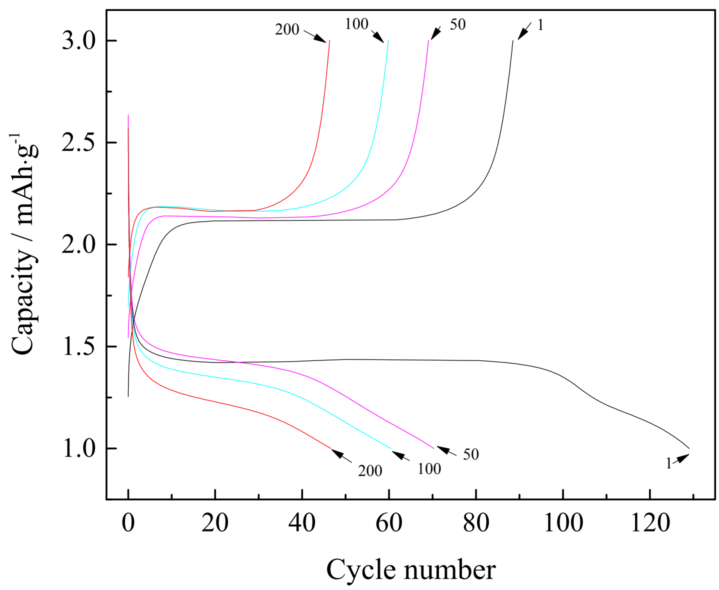

Figure S13. Charge/discharge performance of anatase TiO_2 NTAs in LiTFSI/C_2mimTFSI electrolyte at current rate of 1.5 C.

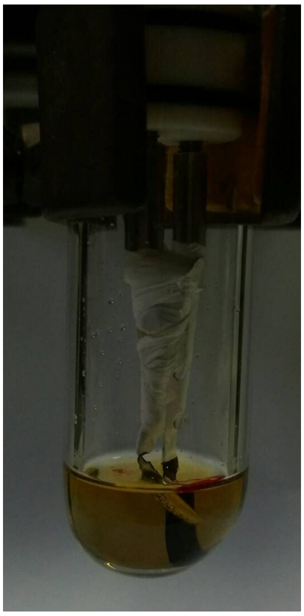

Figure S14. Appearance of LiTFSI/C_2mimTFSI after 200 cycles (cell changed the color from colorless to yellow).

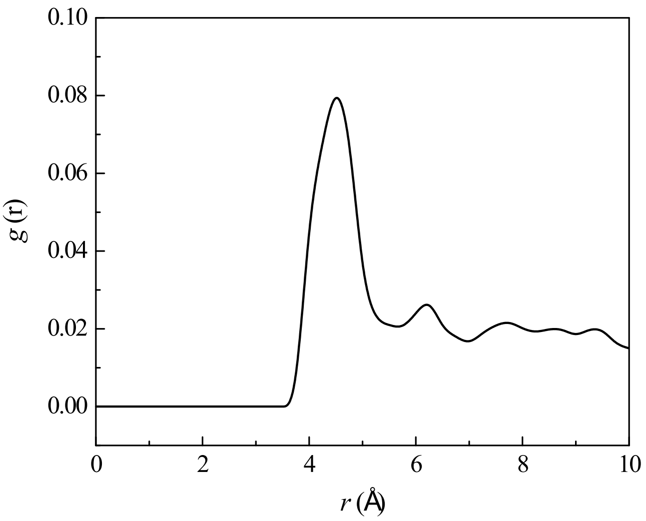

Figure S15. RDF for CH_3 –C(2) from C_2mim^+ and carbonyl oxygen from GBL.